Dynamic Breathing of CO_2 by Hydrotalcite

Shinsuke Ishihara,*,[†] Pathik Sahoo,[†] Kenzo Deguchi,[‡] Shinobu Ohki,[‡] Masataka Tansho,[‡]
Tadashi Shimizu,[‡] Jan Labuta,[†] Jonathan P. Hill,[†] Katsuhiko Ariga,[†] Ken Watanabe,[†] Yusuke Yamauchi,[†]
Shigeru Suehara,[§] and Nobuo Iyi*,[†]

[†]International Center for Materials Nanoarchitectonics (MANA), National Institute for Materials Science (NIMS), 1-1 Namiki, Tsukuba, Ibaraki 305-0044, Japan
[‡]High Field NMR Group, National Institute for Materials Science (NIMS), 3-13 Sakura, Tsukuba, Ibaraki 305-0003, Japan
[§]Material Properties Theory Group, National Institute for Materials Science (NIMS), 1-1 Namiki, Tsukuba, Ibaraki 305-0044, Japan

ⓢ *Supporting Information*

ABSTRACT: The carbon cycle of carbonate solids (e.g., limestone) involves weathering and metamorphic events, which usually occur over millions of years. Here we show that carbonate anion intercalated layered double hydroxide (LDH), a class of hydrotalcite, undergoes an ultrarapid carbon cycle with uptake of atmospheric CO_2 under ambient conditions. The use of ^{13}C-labeling enabled monitoring by IR spectroscopy of the dynamic exchange between initially intercalated ^{13}C-labeled carbonate anions and carbonate anions derived from atmospheric CO_2. Exchange is promoted by conditions of low humidity with a half-life of exchange of ~24 h. Since hydrotalcite-like clay minerals exist in Nature, our finding implies that the global carbon cycle involving exchange between lithosphere and atmosphere is much more dynamic than previously thought.

Figure 1. (a) Dynamic exchange of carbonate anions of LDH with atmospheric CO_2. (b) IR spectra of $^{13}CO_3^{2-}$–LDH and CO_3^{2-}–LDH. (c) Variation of IR frquency of $^{13}CO_3^{2-}$–LDH upon exposure to air at different relative humidities. Note that dry N_2 containing 397 ppm CO_2 was used in place of dry air (relative humidity =5 ± 2%). Air bubbled through water was used as wet air (relative humidity = 98 ± 2%).

The carbon cycle is the biogeo-chemical process by which carbon circulates between the atmosphere, oceans and lithosphere, and includes fossil fuel deposits and the biosphere of Earth.[1] The lithosphere contains by far the largest quantity of carbon, more than 60,000,000 gigatons in the form of sedimentary carbonates, relative to the other carbon pools (720 gigatons in the atmosphere, 38,400 gigatons in the oceans).[1] The carbon cycle involving geological carbon of the lithosphere is based on weathering and metamorphic events so that, despite its extent, its processes are considered to be very slow, occurring on the time scale of millions of years.[2]

Here we show that carbonate anions intercalated within layered double hydroxide (LDH), a class of hydrotalcite, undergo an unusual dynamic exchange with carbonate anions derived from atmospheric CO_2 under ambient conditions (Figure 1a). ^{13}C-labeled carbonate anions ($^{13}CO_3^{2-}$) were used, enabling differentiation by IR spectroscopy between the originally intercalated ^{13}C-labeled carbonate anions and atmospherically-CO_2-derived carbonate anions, which are largely composed of ^{12}C.

Layered double hydroxides (LDHs) compose a class of synthetic clay minerals of general formula $M^{II}_{1-y}M^{III}_y(OH)_2(X^{n-})_{y/n}·mH_2O$, where M^{II}, M^{III}, and X^{n-} are respectively a divalent metal cation, a trivalent metal cation, and a counte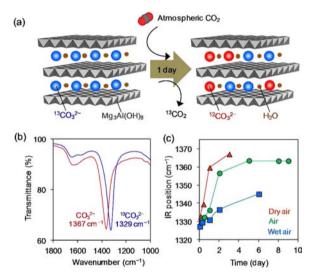ranion, and y is in the range of 0.2−0.33.[3] The typical carbonate-type LDH, $Mg_3Al(OH)_8(CO_3^{2-})_{0.5}·mH_2O$ (CO_3^{2-}–LDH), can be regarded as a two-dimensional (2D) carbonate salt in that it consists of cationic brucite-like oxide layers ($Mg_3Al(OH)_8$), charge-balancing interlayer carbonate anions (CO_3^{2-})$_{0.5}$, and interlayer water (mH_2O). LDHs have attracted interest because of their highly tunable chemical composition,[4] and availability for anion-exchange,[5] catalysts,[6] hybrid materials,[7] etc.

^{13}C-labeled LDH, $Mg_3Al(OH)_8(^{13}CO_3^{2-})_{0.5}·mH_2O$ ($^{13}CO_3^{2-}$–LDH), was synthesized by anion-exchange reaction of chloride-type LDH ($Mg_3Al(OH)_8(Cl^-)·mH_2O$)[8] with ^{13}C-labeled sodium carbonate in water (see Supporting Information [SI]). As shown in Figure 1b, conventional CO_3^{2-}–LDH exhibits C−O stretching (str.) vibration[9] at 1367 cm^{-1}, whereas $^{13}CO_3^{2-}$–LDH exhibits C−O (str.) at 1329 cm^{-1}.[10] This

isotope shift is in agreement with first-principle theoretical calculations (Figure S8, SI). Interestingly, the C−O vibration of $^{13}CO_3^{2-}$−LDH is gradually shifted to higher wavenumber if the sample is left in air (∼24 °C, relative humidity = ∼50%), indicating that $^{13}CO_3^{2-}$ in LDH exchanges with carbonate anions derived from atmospheric CO_2 (Figure 1c, Figure S7, SI). Also, as is shown in Figure 1c, the rate of exchange of carbonate anions is enhanced in dry air (relative humidity = 5 ± 2%) with more than half of $^{13}CO_3^{2-}$ being replaced by $^{12}CO_3^{2-}$ within one day. In contrast, the exchange rate was depressed in wet air (relative humidity = 98 ± 2%) with a corresponding 50% exchange requiring one week. Moreover, when CO_3^{2-}−LDH was dispersed in an aqueous solution of ^{13}C-labeled sodium carbonate, only a slight exchange of carbonate occurred during two weeks (Figure S6, SI). These features indicate that water is a negative factor for exchange of carbonate anions, and that $^{13}CO_3^{2-}$ and $^{12}CO_3^{2-}$ do not undergo a direct exchange process.

In contrast to LDH, the IR spectrum of ^{13}C-labeled sodium carbonate did not vary even after standing open to air for two weeks. Therefore, dynamic exchange of carbonate in air is a characteristic of this LDH. Moreover, we have undertaken an 'accelerated test', in which ^{13}C-labeled sodium carbonate was placed under pure CO_2 (100 kPa) at 150 °C for 3 days (Figure S15, SI). Nevertheless, the IR spectrum of ^{13}C-labeled sodium carbonate only varied slightly. This 'accelerated test' suggests that carbonate anions of sodium carbonate at its exterior surfaces may be slowly exchanging with atmospheric CO_2, while those at the interior cannot.

There have been some reports that calcinated LDHs (so-called, layered double oxides, LDOs, which have different structures from those of the pristine LDHs[11]) can function as high-temperature CO_2 adsorbents,[12] but it is widely considered that pristine LDHs (i.e., noncalcinated LDH) do not possess any CO_2 capture capabilities.[13] In contrast to previous reports, gas adsorption measurements at 25 °C (Figure 2) clearly
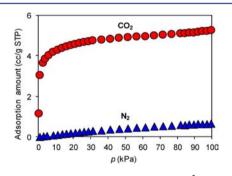

Figure 2. CO_2 and N_2 adsorption isotherms of CO_3^{2-}−LDH at 25 °C. Before measurement, CO_3^{2-}−LDH was thoroughly dried under an N_2 stream to remove loosely bound interlayer water.

indicate that CO_3^{2-}−LDH has a finite capacity (∼4 cc/g at p_{CO2} = 5 kPa) for reversible and selective adsorption of CO_2. Since Mg−OH-rich LDH has been reported to promote base-catalyzed reactions,[14] the adsorption site of CO_2 is probably Mg−OH, where reversible acid−base interactions can occur.

The specific surface area of CO_3^{2-}−LDH was estimated to be 12.3 m^2/g by N_2 adsorption/desorption isotherm at 77.35 K (Figure S13, SI). This value is close to the external surface area of LDH calculated on the basis of the size[3f] and density of LDH (2.03 g/cm^3, Figure S14, SI) so that N_2 cannot enter the interlayer domains. In addition, the shape of the N_2 adsorption/

desorption isotherm can be categorized as being type II, indicating that LDH is neither microporous nor mesoporous. Specific surface area analysis reveals that the external surfaces of LDH crystallites are fully covered by a monolayer of N_2 at ∼5 kPa (indicated by a green arrow in Figure S13b, SI), where ∼2.8 cc/g of N_2 is adsorbed on LDH. In contrast, CO_2 adsorption of LDH at 25 °C (Figure 2) shows that LDH can take up ∼4 cc/g of CO_2, which is a larger molar quantity than that of N_2 adsorption. Moreover, considering that the molecular cross-sectional area of CO_2 (0.210 nm^2 at 273 K) is larger than that of N_2 (0.162 nm^2 at 77 K), it is evident that LDH takes up CO_2 not only at the external surfaces of the crystallites but also at the interlayer nanospace.

Water contents of CO_3^{2-}−LDH ($Mg_3Al(OH)_8(CO_3^{2-})_{0.5}$· mH_2O), determined using thermogravimetry-differential thermal analysis (TG-DTA), were estimated to be m = 2.4 in dry air, 2.54 in air, and 2.9 in wet air (Figures S2, S3, SI). With these water contents m in mind, energy minimized structures of CO_3^{2-}−LDH were constructed in the range m = 2−3 by using density functional theory (DFT) calculations (Figure 3).

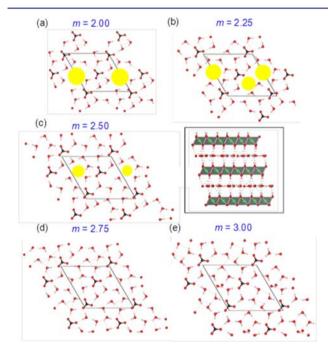**Figure 3.** Energy minimized structures of CO_3^{2-}−LDH (Mg_3Al-$(OH)_8(CO_3^{2-})$·mH_2O) containing various quantities of water m obtained by DFT calculations. Interlayer vacant nanospaces are indicated by yellow circles. Images are viewed along the c axis, while the inset in (c) is along the a axis. Black, red, white, and green balls denote carbon, oxygen, hydrogen, and Mg/Al atoms, respectively.

Interlayer carbonates are hydrogen-bonded to water molecules and the hydroxide layers leading to formation of a 2D carbonate−water network. This result is in agreement with infrared data since the C−O (str.) of $^{13}CO_3^{2-}$−LDH in dry air is at 1328.5 cm^{-1}, whereas the same vibration in $^{13}CO_3^{2-}$−LDH in wet air is at 1326.4 cm^{-1}. The shift can be ascribed to formation of hydrogen bonds between carbonate and water, which tends to decrease the spring constant of the covalent bonds involved. In addition, the calculated interlayer distance of CO_3^{2-}−LDH (7.77 Å for m = 2; 7.78 Å for m = 3) corresponds quite closely with values obtained by XRD (7.81−7.82 Å),

which are hardly influenced by relative humidity (Figure S1, SI).

In Figure 3c (where $m = 2.50$ corresponding to CO_3^{2-}–LDH in dry air) there exist some vacancies in the interlayer H-bonded network (indicated by yellow circles). However, the situation where $m = 3.00$ (corresponding to CO_3^{2-}–LDH in wet air) shown in Figure 3e has all potential H-bonding sites in the interlayer space occupied by water molecules or anions. We believe that this interlayer nanospace is crucial for incorporating CO_2 from air. When the interlayer nanospace is fully occupied by water, atmospheric CO_2 cannot interact with an appropriate adsorption site (such as Mg–OH), so that the rate of carbonate anion exchange is depressed. Thus, the proposed mechanism of the exchange reaction between interlayer carbonate and atmospheric CO_2 is given as follows: (i) atmospheric CO_2 is incorporated into interlayer vacancies contained in the H-bonded interlayer network; (ii) CO_2 reacts with interlayer water to form $2H^+$ and CO_3^{2-}; (iii) interlayer $^{13}CO_3^{2-}$ reacts with $2H^+$ to release $^{13}CO_2$ and water. Deintercalation of CO_3^{2-} mediated by H^+ has already been reported in our previous papers.[3b,8] (iv) CO_3^{2-} remains as a charge balancing interlayer anion.

To investigate this phenomenon further, $^{13}CO_3^{2-}$–LDH was analyzed using solid-state NMR spectroscopy. ^{13}C cross-polarization magic-angle-spinning (CP/MAS) NMR spectra of $^{13}CO_3^{2-}$–LDH (Figure 4a) contain two signals at 170 ppm
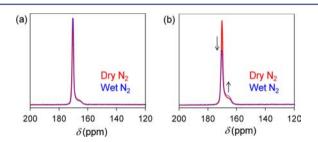

Figure 4. (a) ^{13}C CP/MAS NMR spectra of $^{13}CO_3^{2-}$–LDH. MAS speed was 10 kHz. Contact time and pulse delay were 5 ms and 15 s, respectively. (b) ^{13}C DD/MAS NMR spectra of $^{13}CO_3^{2-}$–LDH was used. MAS speed was 10 kHz. Pulse width and pulse delay were 3 μs and 600 s, respectively. Accumulation was 256 times.

and 167 ppm due to CO_3^{2-} and HCO_3^-, respectively,[15] or CO_3^{2-} coordinated with brucite-like oxide layers in a different manner. Carbonate anions do not contain ^1H atoms which amplify ^{13}C NMR signals in CP mode, so that observation of CP NMR signals indicates that carbonate anions are interacting closely with slow-moving protons contained in water of crystallization and/or hydroxide groups of the brucite-like oxide layers. For quantitative analysis, ^{13}C dipolar decoupled magic-angle-spinning (DD/MAS) NMR of $^{13}CO_3^{2-}$–LDH was also undertaken (Figure 4b). Resonance at 167 ppm increased in intensity when the sample was packed under wet conditions, indicating that the population of the two different states of carbonate anion in LDH is influenced by the quantity of interlayer water. Also, variable-temperature (VT) ^{13}C CP/MAS NMR indicates that the two NMR signals at 170 ppm and 167 ppm are chemically exchangeable (Figure S10, SI).

The T_1 relaxation time of carbonate anions (170 ppm) was around 160 s, which is ~12.5 times shorter than that of ^{13}C-labeled sodium carbonate (~2000 s) measured under identical conditions (Figure S11, SI) clearly indicating that carbonate anions of LDH are more dynamic and energetically active than those of conventional carbonate salts.[16] It can be considered that mobility of carbonate anions in sodium carbonate is restricted due to its 3D lattice structure. Thus, dynamic exchange of carbonate is characteristic of this LDH. This NMR result is in agreement with a synchrotron-radiation XRD study by Sasai et al. which reported that chloride anions incorporated in LDH exhibit abnormally large thermal vibration.[17]

In conclusion, we have demonstrated that carbonate anions within the interlayers of LDH undergo dynamic exchange with carbonate derived from atmospheric CO_2 even under ambient conditions. Rate of exchange is promoted by low relative humidity levels due to the formation of interlayer nanospace vacancies which act as initial points for CO_2 uptake from air. Dynamic exchange of CO_2 arises from the presence of initial points for CO_2 uptake from air and the high activity of interlayer carbonate anions, so that this phenomenon is a characteristic of the structure and chemical properties of LDH. To clarify the initial binding site of CO_2 from air, further study will be needed of the Mg/Al ratio or other metal cations in LDH. Because various hydrotalcite-like clay minerals exist in Nature,[18] the global carbon cycle involving lithosphere and atmosphere could be more dynamic than previously thought. These findings have connotations for studies on CO_2 circulation, global warming, and radiocarbon dating. Finally, the unique interaction between LDH and CO_2 under ambient conditions may be applicable for energy-efficient separations and catalytic conversion of CO_2.

■ ASSOCIATED CONTENT

ⓢ Supporting Information

Materials, synthesis, experimental details, and additional data. This material is available free of charge via the Internet at http://pubs.acs.org.

■ AUTHOR INFORMATION

Corresponding Authors
ishihara.shinsuke@nims.go.jp
iyi.nobuo@nims.go.jp
Notes
The authors declare no competing financial interest.

■ ACKNOWLEDGMENTS

■ REFERENCES

(1) Falkowski, P.; Scholes, R. J.; Boyle, E.; Canadell, J.; Canfield, D.; Elser, J.; Gruber, N.; Hibbard, K.; Högberg, P.; Linder, S.; Mackenzie, F. T.; Moore, B., III; Pedersen, T.; Rosenthal, Y.; Seitzinger, S.; Smetacek, V.; Steffen, W. *Science* **2000**, *290*, 291.

(2) (a) Berner, R. A.; Lasaga, A. C.; Garrels, R. M. *Am. J. Sci.* **1983**, *283*, 641. (b) The Slow Carbon Cycle. http://earthobservatory.nasa.gov/Features/CarbonCycle/page2.php (NASA, accessed 17 Sep 2013).

(3) (a) Layered Double Hydroxide: Jing, H.; Wei, M.; Li, B.; Kang, Y.; Evans, D. G.; Duan, X. *Struct. Bonding (Berlin)* **2006**, *119*, 89. (b) Iyi, N.; Matsumoto, T.; Kaneko, Y.; Kitamura, K. *Chem. Mater.* **2004**, *16*, 2926. (c) Li, L.; Ma, R.; Ebina, Y.; Iyi, N.; Sasaki, T. *Chem. Mater.* **2005**, *17*, 4386. (d) Ma, R.; Liu, Z.; Li, L.; Iyi, N.; Sasaki, T. *J. Mater. Chem.* **2006**, *16*, 3809. (e) Liu, Z.; Ma, R.; Osada, M.; Iyi, N.; Ebina, Y.; Takada, K.; Sasaki, T. *J. Am. Chem. Soc.* **2006**, *128*, 4872.

(f) Okamoto, K.; Sasaki, T.; Fujita, T.; Iyi, N. *J. Mater. Chem.* **2006**, *16*, 1608. (g) Iyi, N.; Kurashima, K.; Fujita, T. *Chem. Mater.* **2002**, *14*, 583. (h) Iyi, N.; Ebina, Y.; Sasaki, T. *J. Mater. Chem.* **2011**, *21*, 8085. (i) Iyi, N.; Ishihara, S.; Kaneko, Y.; Yamada, H. *Langmuir* **2013**, *29*, 2562. (j) Iyi, N.; Ebina, Y.; Sasaki, T. *Langmuir* **2008**, *24*, 5591. (k) Iyi, N.; Tamura, K.; Yamada, H. *J. Colloid Interface Sci.* **2009**, *340*, 67. (l) Ishihara, S.; Iyi, N.; Tsujimoto, Y.; Tominaka, S.; Matsushita, Y.; Krishnan, V.; Akada, M.; Labuta, J.; Deguchi, K.; Ohki, S.; Tansho, M.; Shimizu, T.; Ji, Q.; Yamauchi, Y.; Hill, J. P.; Abe, H.; Ariga, K. *Chem. Commun.* **2013**, *49*, 3631.

(4) (a) Bravo-Suárez, J. J.; Páez-Mozo, E. A.; Oyama, S. T. *Quim. Nova* **2004**, *27*, 601. (b) Ma, R.; Liu, Z.; Takada, K.; Iyi, N.; Bando, Y.; Sasaki, T. *J. Am. Chem. Soc.* **2007**, *129*, 5257. (c) Ishihara, S.; Deguchi, K.; Sato, H.; Takegawa, M.; Nii, E.; Ohki, S.; Hashi, K.; Tansho, M.; Shimizu, T.; Ariga, K.; Labuta, J.; Sahoo, P.; Yamauchi, Y.; Hill, J. P.; Iyi, N.; Sasai, R. *RSC Adv.* **2013**, *3*, 19857.

(5) (a) Bish, D. L. *Bull. Mineral.* **1980**, *103*, 170. (b) Iyi, N.; Sasaki, T. *J. Colloid Interface Sci.* **2008**, *322*, 237. (c) Iyi, N.; Sasaki, T. *Appl. Clay Sci.* **2008**, *42*, 246. (d) Iyi, N.; Yamada, H. *Chem. Lett.* **2010**, *39*, 591. (e) Sasai, R.; Norimatsu, W.; Matsumoto, Y. *J. Hazard Mater.* **2012**, *215−216*, 311.

(6) (a) Cavani, F.; Trifirò, F. F.; Vaccari, A. *Catal. Today* **1991**, *11*, 173. (b) McKenzie, A. L.; Fishel, C. T.; Davis, R. J. J. *J. Catal.* **1992**, *138*, 547. (c) Sels, B.; De Vos, D.; Buntinx, M.; Pierard, F.; Kirsch-De Mesmaeker, A.; Jacobs, P. *Nature* **1999**, *400*, 855. (d) Sels, B. F.; De Vos, D. E.; Jacobs, P. A. *Catal. Rev.* **2001**, *43*, 443. (e) Li, F.; Tan, Q.; Evans, D. G.; Duan, X. *Catal. Lett.* **2005**, *99*, 151. (f) Du, X.; Zhang, D.; Gao, R.; Huang, L.; Shi, L.; Zhang, J. *Chem. Commun.* **2013**, *49*, 6770. (g) He, S.; An, Z.; Wei, M.; Evans, D. G.; Duan, X. *Chem. Commun.* **2013**, *49*, 5912. (h) Teramura, K.; Iguchi, S.; Mizuno, Y.; Shishido, T.; Tanaka, T. *Angew. Chem., Int. Ed.* **2012**, *51*, 8008.

(7) (a) Ogawa, M.; Kuroda, K. *Chem. Rev.* **1995**, *95*, 399. (b) Peak, S.-M.; Oh, J.-M.; Choy, J.-H. *Chem.—Asian J.* **2011**, *6*, 324. (c) Ruiz-Hitzky, E.; Darder, M.; Aranda, P.; Ariga, K. *Adv. Mater.* **2010**, *22*, 323. (d) Káfuňková, E.; Lang, K.; Kubát, P.; Klementová, M.; Mosinger, J.; Šlouf, M.; Troutier-Thuilliez, A.-L.; Leroux, F.; Verney, V.; Taviot-Guého, C. *J. Mater. Chem.* **2010**, *20*, 9423. (e) Bujdak, J.; Iyi, N.; Fujita, T. *Clay Minerals* **2002**, *37*, 121. (f) Ishihara, S.; Iyi, N.; Labuta, J.; Deguchi, K.; Ohki, S.; Tansho, M.; Shimizu, T.; Yamauchi, Y.; Sahoo, P.; Naito, M.; Abe, H.; Hill, J. P.; Ariga, K. *ACS Appl. Mater. Interfaces* **2013**, *5*, 5927.

(8) Iyi, N.; Yamada, H.; Sasaki, T. *Appl. Clay Sci.* **2011**, *54*, 132.

(9) Tossell, J. A. *Inorg. Chem.* **2006**, *45*, 5961.

(10) IR measurements were operated by ATR mode for minimizing the influence from KBr and moisture. See: Iyi, N.; Geng, F.; Sasaki, T. *Chem. Lett.* **2009**, *38*, 808.

(11) (a) Miyata, S. *Clays Clay Miner.* **1980**, *28*, 50. (b) Hibino, T.; Yamashita, Y.; Kosuge, K.; Tsunashima, A. *Clays Clay Miner.* **1995**, *43*, 427.

(12) (a) Miyata, S.; Hirose, T. *Clays Clay Miner.* **1978**, *26*, 441. (b) Hutson, N. D.; Speakman, S. A.; Payzant, E. A. *Chem. Mater.* **2004**, *16*, 4135. (c) Ram Reddy, M. K.; Xu, Z. P.; Lu, G. Q.; Diniz da Costa, J. C. *Ind. Eng. Chem. Res.* **2006**, *45*, 7504. (d) Wang, Q.; Gao, Y.; Luo, J.; Zhong, Z.; Borgna, A.; Guo, Z.; O'Hare, D. *RSC Adv.* **2013**, *3*, 3414.

(13) Gao, Y.; Zhang, Z.; Wu, J.; Yi, X.; Zheng, A.; Umar, A.; O'Hare, D.; Wang, Q. *J. Mater. Chem. A* **2013**, *1*, 12782.

(14) Constantino, V. R. L.; Pinnavaia, T. J. *Inorg. Chem.* **1995**, *34*, 883.

(15) Gottlieb, H. E.; Kotlyar, V.; Nudelman, A. *J. Org. Chem.* **1997**, *62*, 7512.

(16) Hayashi, S.; Suzuki, K.; Hayamizu, K. *J. Chem. Soc., Faraday Trans. 1* **1989**, *85*, 2973.

(17) Sasai, R.; Matsuoka, Y.; Sato, H.; Moriyoshi, C.; Kuroiwa, Y. *Chem. Lett.* **2013**, *42*, 1285.

(18) For example, desautelsite (Mg/Mn-type), pyroaurite (Mg/Fe-type), stichtite (Mg/Cr-type), takovite (Ni/Al-type), and zaccagnaite (Zn/Al-type).